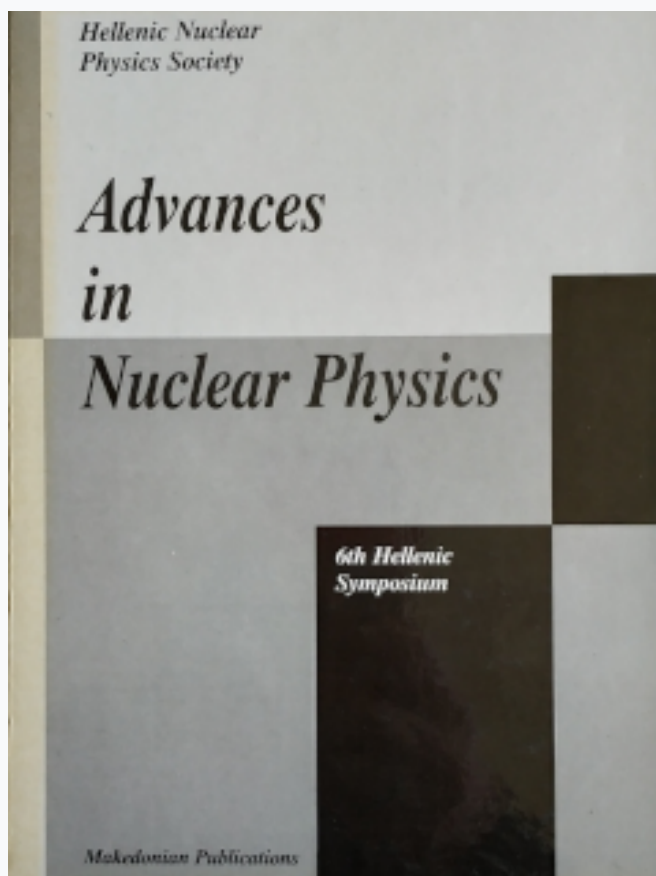


## HNPS Advances in Nuclear Physics

Vol 6 (1995)

HNPS1995



### The Energy Dependence of the Proton-Alpha Reaction to Continuum States

*P. Demetriou*

doi: [10.12681/hnps.2932](https://doi.org/10.12681/hnps.2932)

#### To cite this article:

Demetriou, P. (2020). The Energy Dependence of the Proton-Alpha Reaction to Continuum States. *HNPS Advances in Nuclear Physics*, 6, 253–262. <https://doi.org/10.12681/hnps.2932>

# The Energy Dependence of the Proton-Alpha Reaction to Continuum States

P. Demetriou

*Nuclear Physics Laboratory, Physics Department, University of Oxford, Oxford, U.K.*

---

## Abstract

The energy dependence of the  $(p, \alpha)$  reactions to the continuum states is studied using the Feshbach-Kerman-Koonin multistep theory for the pre-equilibrium reactions assuming the knockout model and using the Hauser-Feshbach theory for the compound nucleus reactions. The energy dependence of the parameter  $W_0$  is related to that of the strength of the effective proton-alpha interaction and hence to that of the alpha-particle optical potential. The formalism is extended to include reactions in which the proton is unbound, and this improves the fit to the experimental data.

---

## 1 Introduction

At low energies nucleon-alpha reactions proceed predominantly to discrete states of the residual nucleus, and these have been extensively studied using the pick-up and knock-out models [5], while at higher energies the reaction proceeds increasingly to unresolvable continuum states. Such reactions are dominated at low energies by the compound nucleus process and as the energy increases the contribution of pre-equilibrium processes become increasingly important. Many analyses of the nucleon-alpha reactions have been made using the [10] and [6] theories for the compound nucleus emission and by a variety of semi-classical exciton models for the pre-equilibrium reactions. Most of these analyses are confined to rather few energies, so we aim to provide a consistent analysis over the whole available energy range using the fully quantum-mechanical multistep theory of Feshbach, Kerman and Koonin [4] (FKK) for the pre-equilibrium reactions, and thus to show in detail how the contributions of the various processes vary with the incident nucleon energy.

In order to separate the compound nucleus and multistep direct contributions to the reaction we use the subtraction method of [2] which requires double differential cross-sections. We select for analysis the data of [0] for  $(p, \alpha)$

reactions from 19.9 to 44.3 MeV on a range of nuclei. Examination of energy spectra shows a large peak at the lower outgoing energies due to compound nucleus emission, a broad shoulder at intermediate energies due to multistep direct reactions and finally a region corresponding to the excitation of discrete states in the residual nucleus. Our principal interest is in the intermediate energy region corresponding to the multistep direct reactions, which is confined by the compound nucleus emission at low energies and by the discrete reactions at high energies. The extent of these energy regions depends on the incident energy and the target mass, and the analysis of the multistep direct reaction is only practicable if the intermediate energy region extends over at least 5 MeV. As the incident energy decreases the regions move together and so the analysis becomes impossible below about 20 MeV for medium weight nuclei. The Coulomb field increases this limit for heavier nuclei. We therefore expect our analysis to give better results for  $^{93}\text{Nb}$  than for the heavier nuclei.

In a previous paper [9] we showed that the  $(p, \alpha)$  reaction at 30 and 44 MeV on several nuclei can be well described by the compound nucleus and FKK multistep direct reactions. In this paper we describe the results of analyses of the same data over a wider range of energies, in order to determine the energy variation of the reaction and in particular to see if it can be linked to that of the alpha-particle optical potential. This work is described in Section 2. In the previous paper it was assumed that the incident proton is captured to form a bound state of the residual nucleus; this is justified at lower incident energies but as the energy increases it becomes increasingly likely that the proton is unbound. The formalism has therefore been extended to include this possibility, as described in Section 3. The remainder of the formalism used is described in the previous paper, which also gives the reasons for assuming that the pre-equilibrium reaction to the continuum takes place predominantly by the knock-out process. Our conclusions are given in Section 4.

## 2 The Energy Dependence

The cross-sections of the  $(p, \alpha)$  reaction at several energies from 19.9 to 44.3 MeV on  $^{93}\text{Nb}$  were analysed by the method described by [9]. It is assumed that the reaction takes place by the knock-out process, and the double-differential cross-sections were calculated using the theory of Feshbach, Kerman and Koonin using a zero-range effective proton-alpha interaction. The contribution of multistep direct (MSD) reactions was found by the subtraction method [2].

The analysis of [9], showed that the value of the overall normalisation constant  $W_0$  is quite sensitive to the optical potentials used, even though they all fit the appropriate elastic scattering data. It is important to reduce this uncertainty,

and we therefore seek some additional constraints on the optical potentials. It has recently been shown by [7] that the scattering matrix elements fitting the elastic scattering cross-section do not necessarily fit the reaction cross-section; this is because the elastic scattering determines only a subset of the scattering matrix elements and the reaction cross-section is also sensitive to others. To fix the optical potential it is therefore necessary to use reaction data as well. We therefore impose the additional requirement that our optical potentials fit the  $(p, \alpha)$  angular distributions as well as the appropriate proton and alpha elastic scattering data. To do this we made calculations with several sets of proton and alpha-particle optical potentials and we selected the combination of the proton potential of [1] and the alpha-particle potential of [8] as giving the best overall fit to the shape of the angular distributions and use this in the analyses at all energies.

We also studied the usefulness of imposing the further requirement that the strength of the incident scattering potential is equal to the final bound-state potential, which follows from the application of the Born Approximation to the quantum-mechanical scattering theory. It was found that this also favours the potential combination mentioned above.

Using these potentials, the data were analysed using the subtraction method, and the results are shown in Fig 1. The overall normalisation is determined by the adjustable parameter  $W_0$ , and the values obtained are given in Table 1.

We next compared the angle-integrated cross-sections with the experimental energy spectra and the results are shown in Fig 2. As in the previous analysis, the data at intermediate outgoing energies are attributable to the MSD reaction, and the large peak at lower energies to compound nucleus emission. These analyses gave a good overall account of the data at the four higher energies, but encountered several difficulties at the two lowest energies of 19.9 and 24.6 MeV: the angular distributions are not well fitted and the predicted values of the angle-integrated cross-sections are too high. It is likely that the reason for this behaviour is the failure of the model at lower energies due to strong coupling to collective states via the inelastic channels. A full coupled reaction channel analysis which would determine such strong-coupling effects on the optical potential is beyond the scope of the present work. However, a qualitative indication of the effect of such coupling can be found through the dispersion relations which show that it is equivalent to adding a surface-peaked term to the real part of the potential, thus increasing its radius.

Calculations were therefore made with proton and alpha-particle optical potentials with a larger radius, and it was indeed found that slightly increasing the proton radius does give a better description of the angular distributions whereas doing the same for the alpha-particle potentials has little effect.

The multistep direct contributions may also be obtained from the optimum fit to the energy spectra, and these are also shown in Fig 2 and the corresponding values of  $W_0$  are included in Table 1. Since the subtraction method is sensitive to the quality of the angular distributions, and hence to the optical potentials, we consider that although the two methods give fairly consistent results within the statistical uncertainties, the results of the best fits to the angle-integrated energy spectra are more reliable than those of the subtraction method and so it is these values we use from hereon.

The values of the parameter  $W_0$  obtained at different incident energies by fitting the angle-integrated cross-sections (Table 1, (b)) are plotted in Fig 3 as a function of incident energy. The energy variation of  $W_0$  is found by fitting a linear function of energy through the given points. For  $^{93}\text{Nb}$  this gives

$$^{93}\text{Nb } W_0 = (69.3 \pm 4.5) - (0.21 \pm 0.09)E \quad (1)$$

For the reasons discussed in Section 1 the values of  $W_0$  for the two lowest incident energies for  $^{93}\text{Nb}$ , are unreliable and thus are not included in the fitting procedure.

In the case of reactions to discrete states, the direct cross-section can be factorised into an energy-independent part depending on the structure of the initial and final states and an energy-dependent factor depending on the reaction mechanism. For reactions to the continuum  $W_0$  can be defined as an average of the structure constant  $\bar{F}(N, Z)$  multiplied by a term depending on energy

$$W_0(E, N, Z) = \bar{F}(N, Z)V_{p\alpha}(E) \quad (2)$$

where the factor  $\bar{F}(N, Z)$  includes a normalising constant and the spectroscopic amplitudes and therefore all the information on the structure properties of the initial and final nuclei. According to the simple folding model, the effective nucleon-alpha interaction  $V_{p\alpha}(E)$  has the same energy dependence as the corresponding optical potential, in this case the alpha-particle optical potential, so we identify  $V_{p\alpha}(E)$  with the strength of that interaction. The energy variation of the real optical potential we have used [8] is

$$V_{OP}^\alpha(E) = (155.1 \pm 28.5) - (0.25 \pm 0.05)E \quad (3)$$

which is consistent with that found for  $W_0$  for  $^{93}\text{Nb}$ .

The folding model relates the strength of the effective proton-alpha interaction  $V(|\vec{r} - \vec{r}_\alpha|)$  to the real part of the alpha-particle optical potential

$$\int \text{Re}U(r_\alpha)d\vec{r}_\alpha = A_T \int V(|\vec{r} - \vec{r}_\alpha|)d\vec{r}. \quad (4)$$

Assuming a zero-range interaction

$$V(|\vec{r} - \vec{r}_\alpha|) = \frac{4\pi}{3} r_0^3 V_{p\alpha} \delta(\vec{r} - \vec{r}_\alpha) \quad (5)$$

and that the real part of the alpha-particle optical potential is given by a Wood-Saxon radial factor  $f(r)$  with the parameters determined by [8] we obtain the values of  $V_{p\alpha}(E)$  presented in Table 2.

The corresponding values for  $\bar{F}(N, Z)$  are then calculated from relation (1) using the values of  $W_0$  given by the best fit energy variations and are also included in Table 2.

### 3 Reactions to Unbound Final States

The analysis of [9] assumed that the proton is captured to a bound state of the residual nucleus. As the incident energy increases it becomes increasingly likely that it will be unbound, so this possibility was included in the theory. For calculational convenience we represent the unbound proton wavefunction by quasi-bound wavefunctions calculated using a Woods-Saxon potential with a small binding energy (0.2 MeV). We therefore use the standard DWBA formalism for a single transition and essentially increase the depth of the potential so as to bind the high-lying states as well.

By allowing the proton to occupy unbound states a larger number of transitions is included in the cross-sections to the continuum region. The level densities of the residual nucleus now correspond to those of proton-particle and alpha-hole state without the restriction that they are bound and therefore are calculated by using the Williams formula [11]. As a result the magnitude of the cross-section for the alpha-particle emission in this energy region increases. These curves give better fits to the data and show the characteristic shoulder that was missing from the results described in Section 2 at energies above 30 MeV. The results are shown in Figs 1-2 (dashed curves). The values of  $W_0$  and  $\bar{F}(N, Z)$  obtained from this analysis are also given in Tables 1 and 2.

### 4 Conclusions

This analysis of  $(p, \alpha)$  reactions to the continuum shows that the reaction proceeds mainly by compound nucleus emission together with a direct component that can be described by the Feshbach, Kerman and Koonin theory of pre-equilibrium emission using the alpha-particle knockout model. The energy variation of the normalising factor  $W_0$  is consistent with that of the real part of

the alpha-particle optical potential, as expected from the folding model. This allows factors that are related to the alpha-particle formation probability to be extracted.

The model was extended to include reactions in which the final proton is unbound, and this markedly improved the fits to the experimental data at the higher incident energies.

## Acknowledgement

PD acknowledges the support of the Greek State Scholarship Foundation.

## References

- [1] Becchetti F D, and Greenlees Jr, G W 1969 *Phys. Rev.* **182** 1190
- [2] Demetriou P, Kanjanarat P and Hodgson P E 1993 *J. Phys. G: Nucl. Part. Phys.* **19** L193; 1994 **20** 1779
- [3] Ferrero A M, Iori I, Molho N and Zetta L 1978 INFN Report INFN/BE 78/6
- [4] Feshbach H, Kerman A K and Koonin S 1980 *Ann. Phys. (NY)* **125** 429
- [5] Gadioli E and Hodgson P E 1992 "Preequilibrium Nuclear Reactions" (Clarendon Press, Oxford)
- [6] Hauser W and Feshbach H 1952 *Phys. Rev.* **87** 366
- [7] Masaki M and Aoki Y 1992 "Annual Report of the Tandem Accelerator Centre", University of Tsakuba, 20; 1993 in: Proc. of the Japan- China Joint Nuclear Physics Symposium "Recent Topics in Nuclear Physics" (Ed. H. Ohnuma and M. Oku) Tokyo Institute of Technology 319
- [8] Nolte M, Machner H and Bojowald J 1987 *Phys. Rev. C* **36** 1312
- [9] Olaniyi H B, Demetriou P and Hodgson P E 1995 *J. Phys. G: Nucl. Part. Phys.* **21** 361
- [10] Weisskopf V F and Ewing P H 1940 *Phys. Rev.* **57** 472
- [11] Williams F C 1971 *Nucl. Phys. A* **166** 231

Table 1

Values of the parameter  $W_0$  in (MeV) obtained from (a) the subtraction method, (b) fitting the angle-integrated spectra and (c) fitting the energy spectra including unbound final proton states .

| Nucleus          | Energy (MeV) | 30-150 deg | 45-135 deg | 60-120 deg | $W_{0,average}$ (a) | $W_0$ (b) | $W_0$ (c) |
|------------------|--------------|------------|------------|------------|---------------------|-----------|-----------|
| <sup>93</sup> Nb | 19.9         | 62.3       | 62.9       | 90.9       | 70±7                | 38±4      |           |
|                  | 24.6         | 52.6       | 62.9       | 84.8       | 67±9                | 30±3      |           |
|                  | 29.7         | 54         | 59.6       | 103        | 68±13               | 68±7      |           |
|                  | 34.6         | 42.4       | 60         | 88.2       | 57±9                | 57±6      | 23.2±2    |
|                  | 41.7         | 42         | 73.4       | 69.7       | 59±10               | 59±6      | 26.8±3    |
|                  | 44.3         | 58.4       | 92.9       | 86.9       | 78±8                | 63±6      | 32.8±3    |

Table 2

Values of the strength  $V_{p\alpha}$  of the effective proton interaction calculated from eq. (4) and the factor  $\bar{F}(N, Z)$  evaluated from eq. (1) for (a) bound final states only and (b) unbound final states also.

| Nucleus          | Energy (MeV) | $V_{p\alpha}$ (MeV) | $\bar{F}(N, Z)$ (a) | $\bar{F}(N, Z)$ (b) |
|------------------|--------------|---------------------|---------------------|---------------------|
| <sup>93</sup> Nb | 19.9         | 174.5               | 0.373               |                     |
|                  | 24.6         | 173.1               | 0.370               |                     |
|                  | 29.7         | 171.6               | 0.367               |                     |
|                  | 34.6         | 170.2               | 0.364               | 0.136               |
|                  | 41.7         | 168.1               | 0.357               | 0.159               |
|                  | 44.3         | 167.4               | 0.358               | 0.196               |

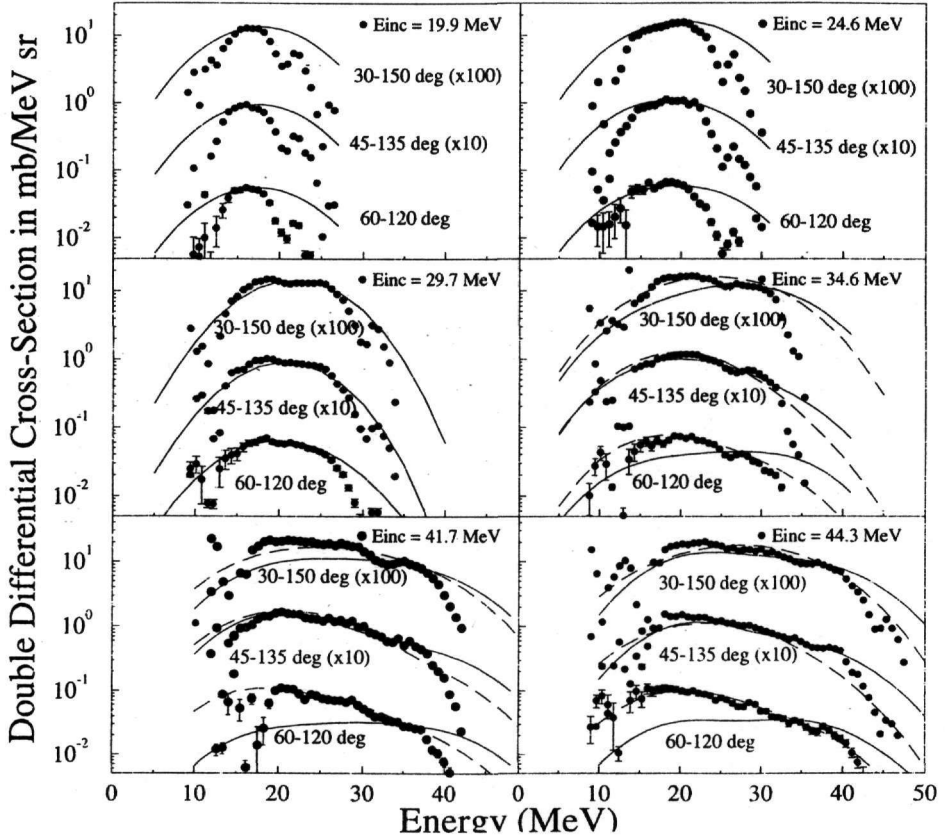


Figure 1: Subtracted double-differential cross-sections for the  $(p, \alpha)$  reaction on  $^{93}\text{Nb}$  at several incident energies [3] compared with similarly-subtracted MSD FKK calculations using the alpha-particle knock-out model with bound final proton states (solid curves) and both bound and unbound proton states (dashed curves). The MSD calculations (only bound final proton states) are normalised to the data using the values  $W_0$  in Table 1.

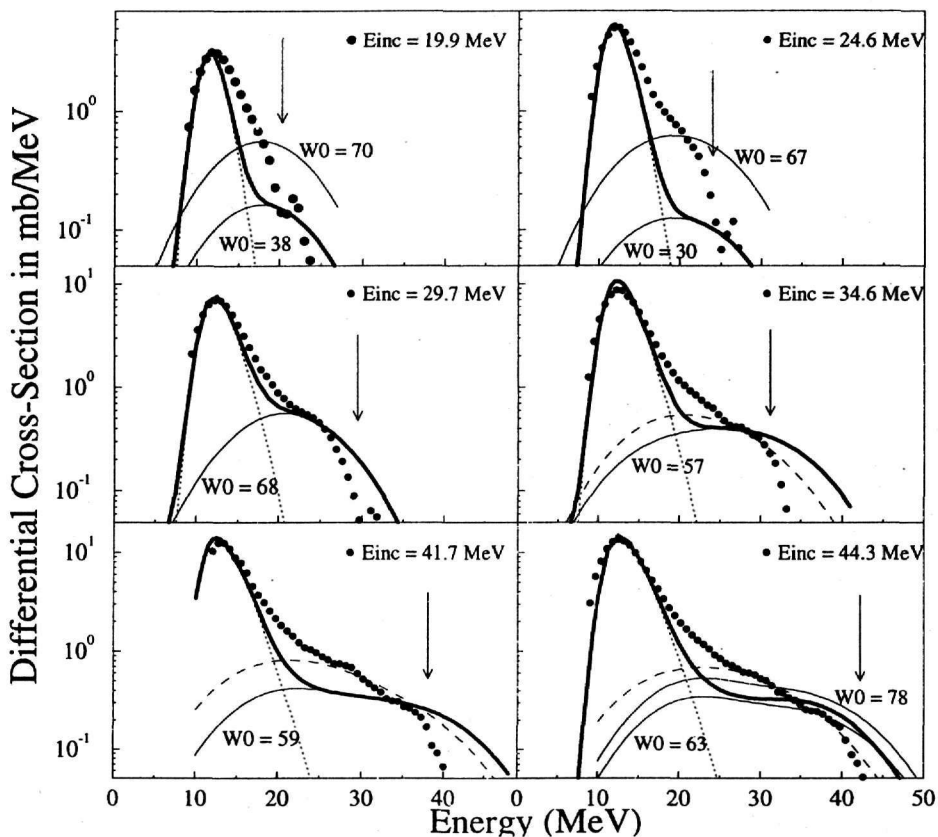


Figure 2: Angle-integrated cross-sections for the  $(p, \alpha)$  reaction on  $^{83}\text{Nb}$  at several incident energies [3] compared with MSD FKK calculations. The thin solid curves obtained with the values of  $W_0$  in Table 1 ((a) and (b)) correspond to bound proton final states only. The dashed curves include both bound and unbound proton states and are normalised using the values  $W_0$ , (c) in Table 1. The arrows indicate the lower limit of the region corresponding to reactions to discrete states.

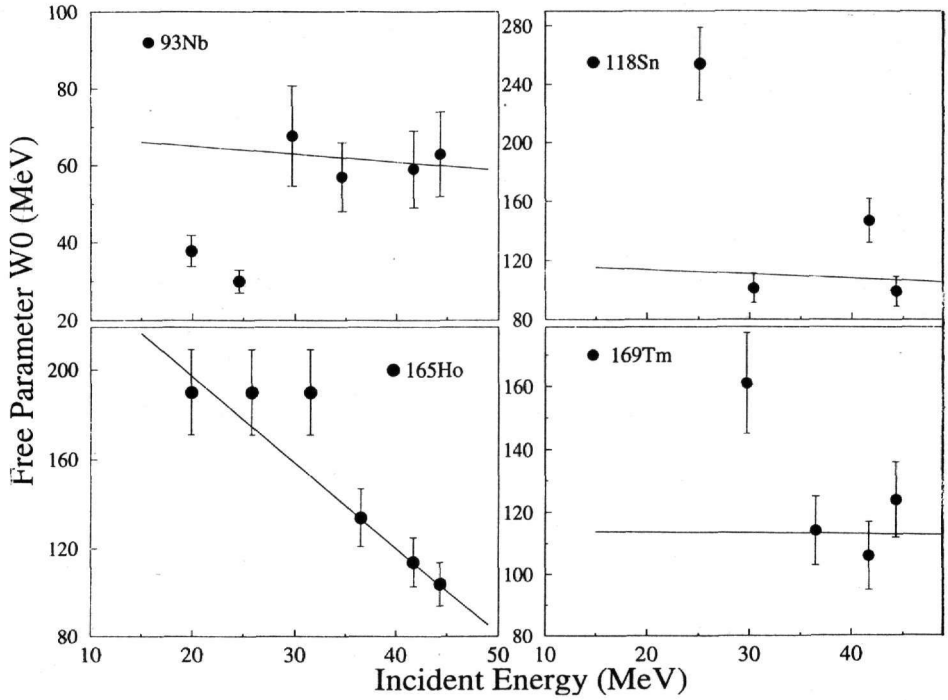


Figure 3: The energy variation of the  $W_0$  values (black circles) of Table 1 (b) fitted with linear curves (solid lines) given by (1) for  $^{93}\text{Nb}$ ,  $^{118}\text{Sn}$ ,  $^{165}\text{Ho}$  and  $^{169}\text{Tm}$ .